Clinical Neurology and Neurosurgery xxx (2012) xxx–xxx

Contents lists available at SciVerse ScienceDirect

Clinical Neurology and Neurosurgery

journal homepage: www.elsevier.com/locate/clineuro

Quantitative evaluation using the plaque/muscle ratio index panels predicts plaque type and risk of embolism in patients undergoing carotid artery stenting

Koichiro Takemoto[a], Tetsuya Ueba[a,*], Koichi Takano[b], Hiroshi Abe[a], Yoko Hirata[c], Toshio Higashi[a], Tooru Inoue[a], Noriyuki Sakata[c], Kengo Yoshimitsu[b]

[a] Department of Neurosurgery, Faculty of Medicine, Fukuoka University, Fukuoka, Japan
[b] Department of Radiology, Faculty of Medicine, Fukuoka University, Fukuoka, Japan
[c] Department of Pathology, Faculty of Medicine, Fukuoka University, Fukuoka, Japan

ARTICLE INFO

Article history:
Received 23 January 2012
Received in revised form 5 November 2012
Accepted 2 December 2012
Available online xxx

Keywords:
Plaque/muscle ratio
MR plaque image
Pathology
Carotid endarterectomy
Carotid artery stenting
Atherosclerosis

ABSTRACT

Objective: We sought to use a magnetic resonance (MR) plaque imaging technique to establish the plaque/muscle ratio (PMR) index panel to identify vulnerable plaques in subjects undergoing carotid artery stenting (CAS).
Methods: Between 2008 and 2010 we treated 69 patients (71 lesions) by elective carotid endarterectomy (CEA) and 35 patients (36 lesions) by CAS. All patients underwent preoperative MR plaque imaging and the ratio of plaque signal intensity to the sternocleidomastoid muscle was calculated. In the CEA group, we categorized the histopathological findings made on the surgical specimens. In the CAS group, we assessed the post-procedure diffusion-weighted images.
Results: PMR index panels for each plaque type were created using the cut-off value obtained from the receiver operating characteristic (ROC) curves of each plaque type. The probability of each of the four plaque types on each panel was assessed by Fisher's exact test. Multinomial logistic regression analysis of the DWI-positive findings determined significant probability ($p = 0.042$).
Conclusion: The results of this study suggest quantitative evaluation using the PMR index panel has a probability to predict both the plaque type and risk of embolism in patients being considered for treatment with CAS.

© 2012 Elsevier B.V. All rights reserved.

1. Introduction

Atherosclerotic carotid plaques are a major cause of cerebral ischemia [1]. The superiority of carotid endarterectomy (CEA) over pharmaceutical treatments has been confirmed [2,3]. High-risk patients considered for CEA can instead be treated by carotid artery stenting (CAS), a minimally invasive treatment modality [4]. However, CAS puts patients with morphologically vulnerable plaques at a higher risk for procedural embolic complications than CEA [5,6].

As the echolucency on carotid ultrasonography (US) is an indicator of soft plaques (lipid or hemorrhagic) and the incidence of ischemic complications during CAS [7,8,9], the accurate preoperative diagnosis of soft plaques is of clinical importance. However, the acquisition of full carotid US images is difficult in patients with a short neck, high carotid bifurcation, or highly calcified plaques [10].

MR plaque imaging studies to characterize the morphology of plaques showed that high-resolution MR imaging was useful [5,11–18]. While MR imaging is a simple, objective, and useful method to diagnose carotid atherosclerosis, few studies have closely assessed the MR imaging signals of plaque components by comparing the results with *in vivo* CEA specimens [13,19–22].

By comparing MR plaque images with the histopathological findings made on CEA specimens we attempted to establish a plaque/muscle ratio (PMR) index panel for high-risk vulnerable plaques. We also evaluated the validity of the PMR index panels for predicting the risk of ischemic complications in patients undergoing CAS.

2. Materials and methods

2.1. Subjects

We analyzed 69 patients (71 lesions) who underwent elective CEA and 35 patients (36 lesions) treated by CAS at our institute between 2008 and 2010. Their age, MRI and histopathological data, degree of stenosis on digital subtraction angiographs, and their

* Corresponding author at: Department of Neurosurgery, Faculty of Medicine, Fukuoka University, 7-45-1 Nanakuma, Jonan-ku, Fukuoka 814-0180, Japan. Tel.: +81 92 801 1011; fax: +81 92 865 9901.
E-mail address: tueba@fukuoka-u.ac.jp (T. Ueba).

0303-8467/$ – see front matter © 2012 Elsevier B.V. All rights reserved.
http://dx.doi.org/10.1016/j.clineuro.2012.12.001

Please cite this article in press as: Takemoto K, et al. Quantitative evaluation using the plaque/muscle ratio index panels predicts plaque type and risk of embolism in patients undergoing carotid artery stenting. Clin Neurol Neurosurg (2012), http://dx.doi.org/10.1016/j.clineuro.2012.12.001

history of stroke, diabetes mellitus, hypertension, and hyperlipidemia were obtained from medical records. The institutional review board of Fukuoka University Hospital approved our study.

2.2. Indications for CEA and CAS

Symptomatic patients were defined as those who had experienced amaurosis fugax, a transient ischemic attack, or a stroke in the territory of the ipsilateral carotid artery within the past 6 months (48 of 71 CEA lesions, 18 of 36 CAS lesions, respectively). The severity of carotid artery stenosis was evaluated by digital subtraction angiography using the North American Symptomatic Trial Collaborators criteria [3]. The rate of stenosis was shown to be 76.6 ± 16.2% (average ± SD) in the CEA group and 76.0 ± 10.5% in the CAS group. The criteria for CEA and CAS treatment included greater than 70% symptomatic and asymptomatic carotid stenosis or greater than 50% symptomatic stenosis with recurrent infarcts on the ipsilateral hemisphere and resistant to maximal medical treatment. With respect to the selection of CEA and CAS, we selected CEA as the first line of treatment for high-risk patients, including those with radiation-induced lesions, restenosis after a prior CEA, and those in whom it was difficult to introduce general anesthesia. We also made an effort not to perform CAS in PMR lesions greater than 1.5 on the T1-PMR (described in greater detail below).

2.3. MRI protocol

All patients were referred for MR plaque imaging within 2 weeks of CEA or CAS. Scans were performed on a 1.5T scanner (ACHIEVA; Philips Medical Systems, Best, the Netherlands) using a SENSE head/neck coil with a quadrate head part with two neck elements. A chemical shift selective fat suppression of spectral presaturation with inversion recovery (SPIR) was applied to all carotid black blood sequences. We obtained short-axis 2D-turbo spin echo (TSE) T1- and T2-weighted images (WI) with the following parameters: TR/TE/TI/echo train length/number of excitations = 600–1000/7/263–399/7/2, matrix size of 320 × 320, a reconstruction matrix of 512 × 512, with a 200 mm-field of view. Four transaxial slices with an interslice gap of 3 mm were obtained. The scan time ranged from 181 to 244 s (T1-WI), and from 193 to 244 s (T2-WI.) Whole-brain single-shot, spin-echo, echo-planar, diffusion-weighted images (DWI) were obtained either on a Philips Achieva 1.5T or an Intera 1.0T scanner.

2.4. Image review

The plaque signal intensity (SI) was made with reference to the immediately adjacent sternocleidomastoid (SCM) muscle. The values were calculated as the signal ratio of the plaque to the SCM and defined as the plaque/muscle ratio (PMR). We used the slice exhibiting the most severe degree of stenosis to record the plaque SI on the short-axis 2D-TSE T1- and T2-WI. In plaques with a heterogeneous intensity, we used the highest intensity component (Fig. 1).

2.5. Histology

Specimens from the CEA group were fixed with 10% buffered formalin, cut into 2 mm serial transverse slices, decalcified, and embedded in paraffin. Microscopic sections (3 μm) were cut from the paraffin-embedded tissue samples and stained with hematoxylin and eosin (H&E), Masson trichrome, and elastica van Gieson stains. The slides were independently evaluated by two reviewers (Y.H. and N.S.) blinded to the imaging results and categorized according to the histopathological classification of Stary et al. [23].

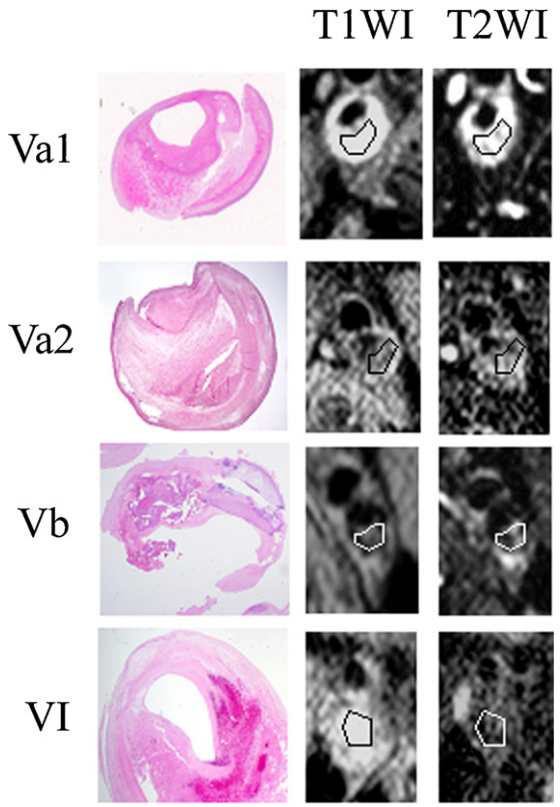

Fig. 1. The modified Stary classification of plaques. Type Va1 lesions manifest as fibrous connective tissue layers with predominant atheroma (>50%); in type Va2 lesions, there is a predominance of connective tissue in fibrous connective tissue layers. Type Vb lesions exhibit a predominant calcification with a fibrolipid lesion. Type VI lesions exhibit hematoma, hemorrhage, or thrombotic deposits on the disrupted surface and are considered complicated lesions.

2.6. Histopathological classification

Type I and II lesions are considered to be early lesions, while Types III, IV, and V are advanced lesions. Type III is characterized by pools of extracellular lipid (pre-atheroma), type IV lesions contain a core of extracellular lipids (atheroma), and type Va lesions exhibit fibrous connective tissue layers plus one or more lipid cores that may be labeled as fibroatheroma. Type Vb lesions are characterized by predominant calcification of a fibrolipid lesion, while type Vc lesions are characterized by fibrous tissue layers, with minimal or even absent lipid and calcium (no core). Type VI lesions are considered to be complicated, exhibiting a disrupted lesion surface, hematoma or hemorrhage, or thrombotic deposits. Type Va (fibroatheroma) plaques include both atheroma-predominant and connective tissue-predominant lesions, thus suggesting that they may differ with respect to plaque instability. Therefore, we separated type Va lesions into two sub-types, Va1, atheroma-predominant (atheroma > 50%) and Va2, connective tissue-predominant plaques (Fig. 1).

2.7. Statistical analysis

The variables in the two distribution groups were compared using the Student's *t*-test and the Fisher's exact test as appropriate. The patients' age, T1- and T2-PMR, and the % of stenosis were handled as continuous variables. The patients' gender and past history of diabetes mellitus, hypertension, hyperlipidemia, or stroke, were handled as categorical variables. PMR index panels for each plaque type were created using the cut-off value obtained with the receiver operating characteristic (ROC) curves for each

Please cite this article in press as: Takemoto K, et al. Quantitative evaluation using the plaque/muscle ratio index panels predicts plaque type and risk of embolism in patients undergoing carotid artery stenting. Clin Neurol Neurosurg (2012), http://dx.doi.org/10.1016/j.clineuro.2012.12.001

Table 1
Patient characteristics treated by CEA and CAS.

	CEA	CAS	*p*
Number of subjects	69	35	
Number of lesions	71	36	
Age	71.5 (6.8)	70.0 (5.6)	0.263*
Gender	M 56:F 12	M 32:F 4	0.570
T1 PMR	1.36 (0.33)	1.30 (0.32)	0.372*
T2 PMR	2.54 (1.02)	2.79 (0.99)	0.235*
% stenosis (NASCET)	76.7 (16.2)	76.6 (11.1)	0.981*
Past history of DM	28 (39.4%)	18 (50.0%)	0.310
Past history of HT	43 (60.6%)	27 (75.0%)	0.197
Past history of HL	46 (64.8%)	27 (75.0%)	0.380
Symptomatic lesion	48 (67.6%)	20 (55.6%)	0.138
Pathology			
Classification of the plaques		NA	NA
Va	14 (19.7%)		
Va1	8 (11.3%)		
Va2	6 (8.5%)		
Vb	8 (11.3%)		
Vc	0 (0.0%)		
VI	49 (69.0%)		

NA: not available; *p*-values were calculated by Fisher's exact test.
* Means calculated by *t*-test.

plaque type. The probability of each of the four plaque types in each panel was assessed by Fisher's exact test. The probability of four panels (as explanatory variables) to DWI-positive complications (as responsive variables) was analyzed by multinomial logistic regression analysis. To evaluate whether the T1- and T2-PMR attributed to DWI-positive complications, the T1- and T2-PMR values were put into the logistic regression analysis as explanatory variables. Differences were considered statistically significant at $p < 0.05$. All analyses were performed using the SPSS 14.0.J software program.

3. Results

3.1. Characteristics of the study population

The two groups did not differ significantly, as shown in Table 1.

3.2. Histological findings

Of the 71 CEA specimens, 8 (11.3%) were characterized as type Va1, 6 (8.5%) as type Va2, 8 (11.3%) as type Vb, and 49 (69%) as type VI lesions (Fig. 1 and Table 1). There were no type Vc lesions.

3.3. T1- and T2-PMR index panels for each plaque type

Type Va1 (atheroma-predominant) lesions had a mean T1- and T2-PMR of 1.63 (0.18) and 2.87 (0.70), respectively. The cut-off value from the ROC curve for type Va1 lesions exceeded 1.51 for the T1-PMR, with a sensitivity of 75.0% and a specificity of 73.0% ($p = 0.004$, Table 2). The T2-PMR was not significant in the ROC analysis. The areas with a T1-PMR greater than 1.51 were assigned to panel A (Fig. 2a). Lesions assigned to panel A were characterized as type Va1 (Fisher's exact test, $p < 0.001$, Table 3).

Type Va2 (connective tissue-predominant) lesions had a mean T1- and T2- PMR of 1.04 (0.17) and 2.59 (0.57), respectively. The cut-off value from the ROC curve for type Va2 lesions was less than 1.18 for the T1-PMR, with a sensitivity of 78.5% and a specificity of 83.3% ($p = 0.004$, Table 2). The T1-PMR between type Va1 and Va2 lesions was significantly different (Student's *t*-test, $p < 0.001$). The areas with a T1-PMR below 1.18 and a T2-PMR more than 1.81 were assigned to panel C (Fig. 2a). Although the assessment of the T2-PMR was not significant by ROC analysis, the 1.81 cut-off value was used to discriminate between type Va2 and Vb lesions. The lesions assigned to panel C were characterized as type Va2 (Fisher's exact test, $p < 0.001$, Table 3).

Type Vb (calcified) lesions had a mean T1- and T2-PMR of 0.85 (0.33) and 1.35 (0.48), respectively. The cut-off value from the ROC curve for type Vb lesions was less than 1.18 for the T1-PMR, with a sensitivity of 81.0% and a specificity of 87.5% ($p = 0.004$, Table 2). The T2-PMR between type Va2 and Vb lesions was statistically significant (Student's *t*-test, $p < 0.001$). The areas with a T1- and T2-PMR below 1.18 and 1.81, respectively, were assigned to panel D (Fig. 2a). The lesions assigned to panel D were characterized as type Vb (Fisher's exact test, $p < 0.001$, Table 3).

Type VI (complicated) lesions had a mean T1- and T2-PMR of 1.44 (0.26) and 2.68 (1.04), respectively. The cut-off value from the ROC curve for type VI lesions was greater than 1.18 and less than 1.51, with a sensitivity of 85.7% and a specificity of 59.1% ($p = 0.016$, Table 2). The T2-PMR was not significant by ROC analysis. The areas with a T1-PMR more than 1.18 and less than 1.51 were assigned to panel B (Fig. 2a). The lesions assigned to panel B tended to be type VI (Fisher's exact test, $p = 0.082$, Table 3).

Table 3
Prediction of each plaque type based on PMR index panels.

Panel	Plaque type			
	Va1	VI	Va2	Vb
A	$p = 0.001$	–	–	–
B		$p = 0.082$*	–	
C	–	–	$p < 0.001$	–
D	–	–		$p < 0.001$

Fisher's exact test was performed; * means not significant because type VI plaques were widely distributed on panels A and B.

3.4. Post-CAS positive diffusion-weighted images (DWI)

The distribution of the T1- and T2-PMR in the CAS group is shown on the PMR index panels (Fig. 2b). Following the completion of all the procedures, with the aid of embolic protection systems, all patients treated by CAS underwent DWI on days 1 through 7. Of the

Table 2
Cut-off values for each plaque type based on ROC curves.

		Cut-off	Area	95% CI	*p*-Value	Sensitivity	Specificity
Va1	T1PMR	1.51≧	0.814	0.686–0.943	0.004	75.0%	73.0%
	T2 PMR	–	0.629	0.456–0.802	0.237	–	–
Va2	T1 PMR	1.18<	0.853	0.762–0.944	0.004	78.5%	83.3%
	T2 PMR	–	0.453	0.281–0.625	0.702	–	–
Vb	T1 PMR	1.18<	0.927	0.853–1.000	<0.001	81.0%	87.5%
	T2 PMR	1.81<	0.914	0.838–0.990	<0.001	81.0%	87.5%
VI	T1 PMR	1.18≧	0.680	0.522–0.838	0.016	85.7%	59.1%
	T2 PMR	–	0.616	0.475–0.757	0.120	–	–

(–) means: not significant.

Please cite this article in press as: Takemoto K, et al. Quantitative evaluation using the plaque/muscle ratio index panels predicts plaque type and risk of embolism in patients undergoing carotid artery stenting. Clin Neurol Neurosurg (2012), http://dx.doi.org/10.1016/j.clineuro.2012.12.001

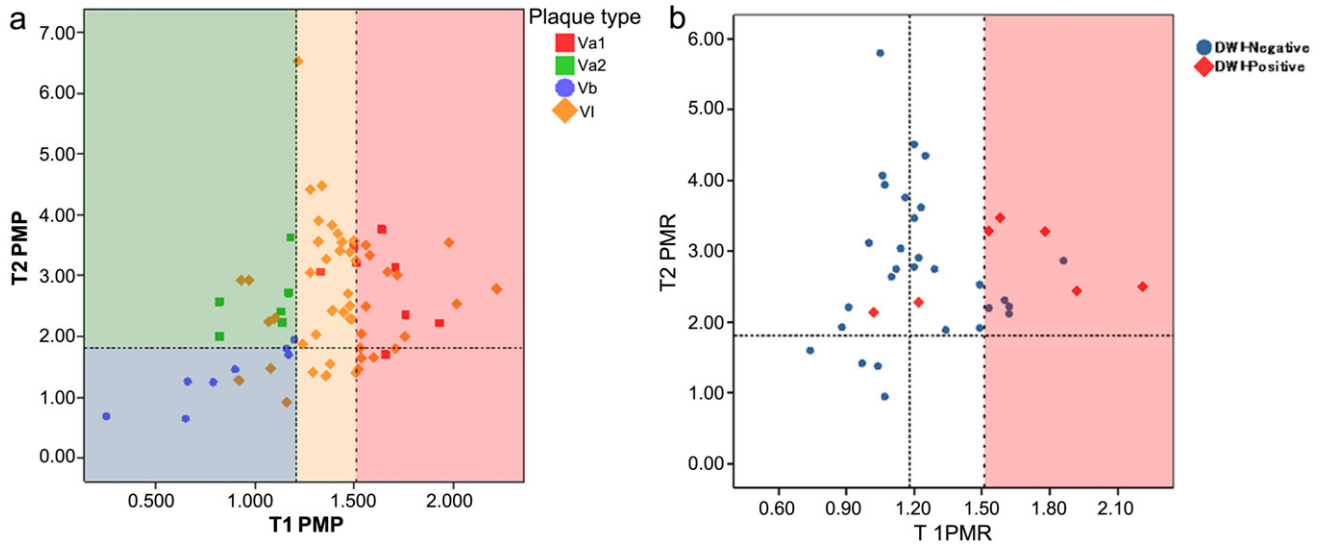

Fig. 2. The distribution of each plaque type based on T1- and T2-PMR cut-off values. (a) The red, orange, and green boxes and blue circles represent type Va1, VI, Va2, and Vb plaques, respectively. Panels A, B, C, and D are shown in red, orange, green and blue, respectively. The vertical dotted lines represent the T1-PMR of 1.51 and 1.18, and the horizontal dotted line represents a T2-PMR of 1.81. (b) Blue circles and red squares represent DWI-negative and DWI-positive findings, respectively. DWI-positive complications were likely to happen from Panel D to A determined by multinomial logistic regression analysis ($p = 0.042$, Table 4).

36 total lesions observed at the ipsilateral ICA territory of the cerebral hemisphere, seven (19.4%) were classified as positive DWI (red squares in Fig. 2b), while two of the 35 patients suffered transient hemiplegia. Debris trapped by the embolic protection system at the end of the procedure was observed in four cases. Although there was no correlation between presence of the debris and the T1-PMR, the T1-PMR in four cases was higher (mean 1.45 ± 0.40), also three cases were presented with positive DWI. The cut-off value from the ROC curve of the DWI-positive lesions exceeded 1.51 in the T1-PMR, with a sensitivity of 71.4% and a specificity of 82.8% ($p = 0.024$, Table 4). The T2-PMR was not significant by ROC analysis. These values were the same for the type Va1 lesions. Multinomial logistic regression analysis determined DWI-positive complications were likely to occur from panels D through A ($p = 0.042$, Table 4). Logistic regression analysis determined a higher T1-PMR in patients presenting with DWI-positive complications (odds ratio 49.9, 95% CI: 2.1–1175.1, $p = 0.015$, data not shown). These findings suggest that type Va1 plaques may be a risk factor for increased complications. In addition, to investigate whether aortic atheromatous plaques contributed to embolic complications, we analyzed the findings using 3D-CT angiography. Four out of seven DWI-positive cases and 13 out of 29 DWI-negative cases had aortic atheromatous plaques. We determined the presence of an aortic atheromatous plaque did not significantly contribute to embolic complications as determined by Fisher's exact test ($p = 0.684$).

Table 4
Plaque cut-off values based on ROC curves and prediction of DWI positive cases after CAS based on PMR index panels.

	Cut-off	Area	95% CI	*p*-Value	Sensitivity	Specificity
T1 PMR	1.51≦	0.778	0.559–0.998	0.024	82.8%	71.4%
T2 PMR	–	0.525	0.456–0.802	0.842	–	–

Panel	Odds	*p*-Value	Likelihood
A	1.1×10^9	<0.001	
B	1.0×10^7	<0.001	
C	1.0×10^7	<0.001	
D	1		$p = 0.042$

(–) means: not significant.

3.5. Post-CEA positive diffusion-weighted images (DWI)

All CEA cases were subjected to MRI both pre- and post-operatively. Five out of the 71 CEA cases had fresh DWI-positive findings preoperatively. There were two additional DWI-positive cases noted after CEA. One case of acute stroke showed an enlarged infarcted area and the other showed a small asymptomatic infarction.

4. Discussion

In this study we demonstrate that the T1- and T2-PMR index panels aid in the histopathological identification of carotid plaques and the risk of embolism in patients scheduled for CAS. Our findings therefore confirm the modified histological classification of atherosclerotic lesions promulgated in 1995 by the American Heart Association [23] is of histopathological and clinical value.

There is an increasing evidence that the morbidity resulting from CAS is related to thrombosis, ulceration, thinned fibrous caps, and intra-plaque hemorrhage [4,8,24,25]. Therefore, it is important to identify patients with high-risk plaques when considering the indications for CAS. MR plaque imaging has been considered to be useful for evaluating the characteristics and vulnerability of plaques [14,18,26–30]. As described by previous studies the imaging methods are divided into three main groups, including "multi-contrast imaging", "single-contrast imaging" and "enhanced-contrast imaging". Multi-contrast imaging, which commonly uses four sequences (such as T1-, T2-, Proton density-WI and TOF), has the possibility of elucidating the nature of the plaque by the combination of the respective signal patterns [11,12,16–19,26,31,32]. Indeed, Cai et al. reported that plaques on high-resolution multicontrast MRI scans correlated with the histological findings [11]. Plaques with a lipid ridge were hyperintense, calcified plaques were hypointense, and fibrous plaques were isointense on T1WI [22]. In our study, the MR signal of fibrous tissue and calcification were also closely correlated with the histological findings. In contrast, the MR signal of intraplaque hemorrhage was variable, possibly reflecting the integrity of the red blood cells and hemoglobin status in the region [26]. Yuan et al. reported that these factors strongly affected tissue T2 relaxation

times but have a smaller impact on the T1WI [17]. A single-contrast image is composed of one sequence and is specific in detecting one phenomenon, while most imaging techniques are modified sequences [13,28,29,33]. Moody and colleagues developed an MR direct thrombus imaging (DTI) technique, with high sensitivity and specificity (84%), which is useful in detecting complicated plaques (American Heart Association (AHA) type VI) [28]. The contrast-enhanced imaging technique is useful to distinguish the fibrous cap and necrotic core accurately [12,34], as well as to detect the intraplaque inflammatory region using targeted molecular and cellular contrast agents [35–38]. Tang et al. evaluated the effect of atorvastatin on carotid plaque inflammation as determined by ultrasmall superparamagnetic iron oxide (USPIO). They reported a significant correlation between aggressive lipid-lowering therapy and a reduction in USPIO-defined inflammation [36].

The quantitative evaluation of plaques using the PMR is suitable as a way to standardize plaque SI on all images. Several studies have used the same method as we did in our present study [22,24,25]. Kashiwagi et al. analyzed the relationship between embolic complications during CAS with MR plaque images and found that patients with a T1-PMR of more than 1.5 were at a significantly higher risk of embolism [25]. Another study by Ishibashi et al. used a different MRI protocol that applied magnetization-prepared rapid acquisition with gradient echo (MPRAGE). They categorized plaques with a T1-PMR of more than 2.0 as high-intensity plaques [24]. In their study, the incidence of embolic complications during CAS was significantly higher in patients with high-intensity plaques compared with iso-intensity plaques (21.1% *vs.* 0%). Finally, Yoshida et al. reported a correlation between the PMR with CEA specimens. When the PMR cutoff value was set at 1.25, it was 79.4% sensitive and 84.4% specific for the diagnosis of soft plaques [22]. These studies are in agreement with our cutoff value findings of 1.18.

We introduced a modified classification of type Va lesions into type Va1 and Va2 lesions based on their histopathology. We used the resulting index panels based on their T1- and T2-PMR, where panels A, B, C, and D correspond to type Va1, VI, Va2, and Vb carotid lesions, respectively. We validated our index panels in 35 patients (36 lesions) who underwent CAS and determined DWI-positive complications most likely to occur from Panel D to A by multinomial logistic regression analysis (Table 4). Therefore, a higher T1-PMR is expected to be present in patients presenting with DWI-positive complications. From our findings we recommend that subjects in panels A and B should undergo CAS with robust antiplatelet and/or anticoagulant therapy. More specific MR imaging modalities need to be developed to better predict the risk of embolism.

4.1. Limitations of this study

Limitations of our study include a small study population, which reduced the power of our statistical analysis and possibly caused a type II error. Therefore, we should not draw conclusions about further treatment guidelines at the present time. Further studies are required for further validation of the T1- and T2-PMR index panels.

5. Conclusion

In conclusion, our histopathological findings indicate the modified classification of type Va1 and Va2 plaques may be of clinical importance. Although the variety of imaging protocols and MRI scanners used for MR plaque imaging may result in different cut-off values, a quantitative evaluation using the T1- and T2-PMR index panels may better identify the histopathological nature of carotid plaques and assist in assessing the risk of embolism in patients being considered for treatment by CAS.

Source of funding

None.

Conflict of interest

None.

References

[1] Barnett HJ, Gunton RW, Eliasziw M, Fleming L, Sharpe B, Gates P, et al. Causes and severity of ischemic stroke in patients with internal carotid artery stenosis. JAMA 2000;283:1429–36.
[2] Rothwell PM, Gutnikov SA, Warlow CP. Reanalysis of the final results of the European Carotid Surgery Trial. Stroke 2003;34:514–23.
[3] Barnett HJ, Taylor DW, Eliasziw M, Fox AJ, Ferguson GG, Haynes RB, et al. Benefit of carotid endarterectomy in patients with symptomatic moderate or severe stenosis, North American Symptomatic Carotid Endarterectomy Trial Collaborators. New England Journal of Medicine 1998;339:1415–25.
[4] Yadav JS, Wholey MH, Kuntz RE, Fayad P, Katzen BT, Mishkel GJ, et al. Protected carotid-artery stenting versus endarterectomy in high-risk patients. New England Journal of Medicine 2004;351:1493–501.
[5] Gronholdt ML, Nordestgaard BG, Wiebe BM, Wilhjelm JE, Sillesen H. Echolucency of computerized ultrasound images of carotid atherosclerotic plaques are associated with increased levels of triglyceride-rich lipoproteins as well as increased plaque lipid content. Circulation 1998;97:34–40.
[6] El-Barghouty NM, Levine T, Ladva S, Flanagan A, Nicolaides A. Histological verification of computerised carotid plaque characterisation. European Journal of Vascular and Endovascular Surgery 1996;11:414–6.
[7] Henry M, Henry I, Klonaris C, Masson I, Hugel M, Tzvetanov K, et al. Benefits of cerebral protection during carotid stenting with the PercuSurge GuardWire system: midterm results. Journal of Endovascular Therapy 2002;9:1–13.
[8] Biasi GM, Froio A, Diethrich EB, Deleo G, Galimberti S, Mingazzini P, et al. Carotid plaque echolucency increases the risk of stroke in carotid stenting: the Imaging in Carotid Angioplasty and Risk of Stroke (ICAROS) study. Circulation 2004;110:756–62.
[9] Ohki T, Marin ML, Lyon RT, Berdejo GL, Soundararajan K, Ohki M, et al. Ex vivo human carotid artery bifurcation stenting: correlation of lesion characteristics with embolic potential. Journal of Vascular Surgery 1998;27:463–71.
[10] Chaudhuri TK, Fink S, Weinberg S, Farpour A. Pathophysiologic considerations in carotid artery imaging: current status and physiologic background. American Journal of Physiologic Imaging 1992;7:77–94.
[11] Cai JM, Hatsukami TS, Ferguson MS, Small R, Polissar NL, Yuan C. Classification of human carotid atherosclerotic lesions with in vivo multicontrast magnetic resonance imaging. Circulation 2002;106:1368–73.
[12] Cai J, Hatsukami TS, Ferguson MS, Kerwin WS, Saam T, Chu B, et al. In vivo quantitative measurement of intact fibrous cap and lipid-rich necrotic core size in atherosclerotic carotid plaque: comparison of high-resolution, contrast-enhanced magnetic resonance imaging and histology. Circulation 2005;112:3437–44.
[13] Hishikawa T, Iihara K, Yamada N, Ishibashi-Ueda H, Miyamoto S. Assessment of necrotic core with intraplaque hemorrhage in atherosclerotic carotid artery plaque by MR imaging with 3D gradient-echo sequence in patients with high-grade stenosis. Clinical article. Journal of Neurosurgery 2010;113:890–6.
[14] Honda M, Kitagawa N, Tsutsumi K, Nagata I, Morikawa M, Hayashi T. High-resolution magnetic resonance imaging for detection of carotid plaques. Neurosurgery 2006;58:338–46 [discussion 338-346].
[15] Quick HH, Debatin JF, Ladd ME. MR imaging of the vessel wall. European Radiology 2002;12:889–900.
[16] Yuan C, Kerwin WS. MRI of atherosclerosis. Journal of Magnetic Resonance Imaging 2004;19:710–9.
[17] Yuan C, Mitsumori LM, Beach KW, Maravilla KR. Carotid atherosclerotic plaque: noninvasive MR characterization and identification of vulnerable lesions. Radiology 2001;221:285–99.
[18] Yuan C, Mitsumori LM, Ferguson MS, Polissar NL, Echelard D, Ortiz G, et al. In vivo accuracy of multispectral magnetic resonance imaging for identifying lipid-rich necrotic cores and intraplaque hemorrhage in advanced human carotid plaques. Circulation 2001;104:2051–6.
[19] Cappendijk VC, Cleutjens KB, Kessels AG, Heeneman S, Schurink GW, Welten RJ, et al. Assessment of human atherosclerotic carotid plaque components with multisequence MR imaging: initial experience. Radiology 2005;234:487–92.
[20] Saam T, Ferguson MS, Yarnykh VL, Takaya N, Xu D, Polissar NL, et al. Quantitative evaluation of carotid plaque composition by in vivo MRI. Arteriosclerosis, Thrombosis, and Vascular Biology 2005;25:234–9.
[21] Takano K, Yamashita S, Takemoto K, Inoue T, Sakata N, Kuwabara Y, et al. Characterization of carotid atherosclerosis with black-blood carotid plaque imaging using variable flip-angle 3D turbo spin-echo: comparison with 2D turbo spin-echo sequences. European Journal of Radiology 2012;81:e304–9.
[22] Yoshida K, Narumi O, Chin M, Inoue K, Tabuchi T, Oda K, et al. Characterization of carotid atherosclerosis and detection of soft plaque with use of black-blood MR imaging. American Journal of Neuroradiology 2008;29:868–74.
[23] Stary HC, Chandler AB, Dinsmore RE, Fuster V, Glagov S, Insull Jr W, et al. A definition of advanced types of atherosclerotic lesions and a histological

classification of atherosclerosis. A report from the Committee on Vascular Lesions of the Council on Arteriosclerosis, American Heart Association. Arteriosclerosis, Thrombosis, and Vascular Biology 1995;15:1512–31.
[24] Ishibashi T, Murayama Y, Saguchi T, Ebara M, Arakawa H, Irie K. Relation between plaque characteristics on MR imaging and distal protection device in predicting risks of thromboembolic events during carotid artery stenting. JNET (Japanese) 2009;3:3–9. http://square.umin.ac.jp/~jsnet/sozai/JNET/3-1/3-1-003.pdf
[25] Kashiwagi J, Kiyosue H, Nakahara I, Matsumoto S, Hitohata M, Abe T. Multicenter analysis of embolic complications during carotid artery stenting using Angioguard XP filter wire – predicting high risk patients by MR plaque image and length of stenosis. JNET (Japanese) 2008;2:179–87. http://www.jsnet.umin.jp/sozai/JNET/2-3/2-3-179F.pdf
[26] Chu B, Kampschulte A, Ferguson MS, Kerwin WS, Yarnykh VL, O'Brien KD, et al. Hemorrhage in the atherosclerotic carotid plaque: a high-resolution MRI study. Stroke 2004;35:1079–84.
[27] Coombs BD, Rapp JH, Ursell PC, Reilly LM, Saloner D. Structure of plaque at carotid bifurcation: high-resolution MRI with histological correlation. Stroke 2001;32:2516–21.
[28] Moody AR, Murphy RE, Morgan PS, Martel AL, Delay GS, Allder S, et al. Characterization of complicated carotid plaque with magnetic resonance direct thrombus imaging in patients with cerebral ischemia. Circulation 2003;107:3047–52.
[29] Murphy RE, Moody AR, Morgan PS, Martel AL, Delay GS, Allder S, et al. Prevalence of complicated carotid atheroma as detected by magnetic resonance direct thrombus imaging in patients with suspected carotid artery stenosis and previous acute cerebral ischemia. Circulation 2003;107:3053–8.
[30] Yamada N, Higashi M, Otsubo R, Sakuma T, Oyama N, Tanaka R, et al. Association between signal hyperintensity on T1-weighted MR imaging of carotid plaques and ipsilateral ischemic events. American Journal of Neuroradiology 2007;28:287–92.
[31] Kampschulte A, Ferguson MS, Kerwin WS, Polissar NL, Chu B, Saam T, et al. Differentiation of intraplaque versus juxtaluminal hemorrhage/thrombus in advanced human carotid atherosclerotic lesions by in vivo magnetic resonance imaging. Circulation 2004;110:3239–44.
[32] Takaya N, Yuan C, Chu B, Saam T, Underhill H, Cai J, et al. Association between carotid plaque characteristics and subsequent ischemic cerebrovascular events: a prospective assessment with MRI-initial results. Stroke 2006;37:818–23.
[33] Hatsukami TS, Ross R, Polissar NL, Yuan C. Visualization of fibrous cap thickness and rupture in human atherosclerotic carotid plaque in vivo with high-resolution magnetic resonance imaging. Circulation 2000;102:959–64.
[34] Sirol M, Itskovich VV, Mani V, Aguinaldo JG, Fallon JT, Misselwitz B, et al. Lipid-rich atherosclerotic plaques detected by gadofluorine-enhanced in vivo magnetic resonance imaging. Circulation 2004;109:2890–6.
[35] Amirbekian V, Lipinski MJ, Briley-Saebo KC, Amirbekian S, Aguinaldo JG, Weinreb DB, et al. Detecting and assessing macrophages in vivo to evaluate atherosclerosis noninvasively using molecular MRI. Proceedings of the National Academy of Sciences of the United States of America 2007;104:961–6.
[36] Tang TY, Howarth SP, Miller SR, Graves MJ, Patterson AJ, Li ZY, et al. The ATHEROMA (Atorvastatin Therapy: Effects on Reduction of Macrophage Activity) Study. Evaluation using ultrasmall superparamagnetic iron oxide-enhanced magnetic resonance imaging in carotid disease. Journal of the American College of Cardiology 2009;53:2039–50.
[37] Trivedi RA, Graves MJ, Cross JJ, Horsley J, Goddard MJ, Skepper JN, et al. In vivo detection of macrophages in human carotid atheroma: temporal dependence of ultrasmall superparamagnetic particles of iron oxide-enhanced MRI. Stroke 2004;35:1631–5.
[38] Winter PM, Morawski AM, Caruthers SD, Fuhrhop RW, Zhang H, Williams TA, et al. Molecular imaging of angiogenesis in early-stage atherosclerosis with alpha(v)beta3-integrin-targeted nanoparticles. Circulation 2003;108:2270–4.

Please cite this article in press as: Takemoto K, et al. Quantitative evaluation using the plaque/muscle ratio index panels predicts plaque type and risk of embolism in patients undergoing carotid artery stenting. Clin Neurol Neurosurg (2012), http://dx.doi.org/10.1016/j.clineuro.2012.12.001